Spectroscopic Study the Air-Processed Degradation Mechanism of Inverted Organic Solar Cells

Minshuai Wang[1]*, Xiaomei Cai[1], Yinghong Huang[1], Kai Zheng[1] and Fumin Li[2]

[1] Department of Physics, School of Science, Jimei University, Xiamen, China, [2] Henan Key Laboratory of Photovoltaic Materials, Henan University, Kaifeng, China

Organic solar cells are promising for the next-generation photovoltaic technology owing to its low cost and flexibility. The possibility of efficient large-area roll-to-roll production has attracted worldwide industrial interest. However, the instability and glove-box process still impede the industrial production of organic solar cells. In this paper, we investigated air-processed degradation mechanisms to provide instructions for practical applications. The air-processed degradation mechanism of the organic solar cells is ascribed that the PEDOT:PSS interfacial layer is oxidized by oxygen and the active layer p-DTS(FBTTh$_2$)$_2$ tends to be affected by water. The air-processed degradation of the PEDOT:PSS interfacial layer results from the oxidation and desulfurization of PEDOT:PSS, which caused huge efficiency loss. The active layer of p-DTS(FBTTh$_2$)$_2$:PC$_{71}$BM tends to be affected by ambient environment, which led to fatal results. The research on these unresolved degradation mechanisms enables us to choose the suitable materials and get stable performance in the air-processed situation.

Keywords: organic solar cell, degradation, X-ray photoelectron spectroscopy, air-processing, spectroscopic techniques

INTRODUCTION

Bulk-heterojunction organic solar cells (BHJ-OSCs) are a superior alternative to silicon-based solar cells with benefits of low cost, light-weight, and large-scale roll-to-roll processing. Over the past few years, the power conversion efficiency (PCE) of OSC devices has been improved enormously to 16.35% [1–5]. Great progress has been achieved through the development of photoactive materials and the improved morphology of the active layer. Recently, Yuan et al. [2] reported a 15.7% PCE of binary OSCs with PM6 as donor and new non-fullerene Y6 as acceptor with near-infrared absorption ability and a good match with efficient polymer donors. Moreover, OPVs made from Y6 and Pt-PSFTZ are reported to exhibit a very high efficiency of 16.35% [5]. This research shows a bright future for practical application of OSC.

Aside from the PCE, there are three important factors: lifetime, cost, and processing technologies and conditions. Long operational lifetimes and cheap cost of solar cell devices are required in practical application. Many studies have been carried out showing that the stability/degradation issue is rather complicated and certainly not yet fully understood though the progress has been made. For organic solar cells, the degradation depends strongly on environmental conditions [6, 7]. Researchers proposed alternative solutions such as using nanocrystalline ZnO interfacial layers, and some other reported methods to improve the OPV cells stability [8–10].

The processing technologies and conditions are also extremely crucial to the practical application of OSC. As for processing conditions, most OPV devices are fabricated in glove-box, owing to their sensitivity to environmental exposure [11, 12]. For example, the oxygen-induced degradation would be expected to have a profound impact on the stability of a wide range of devices such as light-emitting diodes and organic solar cells, which is likely to be the key concern for many practical technology applications. However, the underlying origins of the processing stability have not been elucidated, and little attention has been placed on the degradation mechanism and the importance of different factors. On top of that, the time during spin-coat or blade-coat is only a few minutes, along with 10 min of annealing. It is not easy to figure out the processing degradation or the chemical change process in such a short time. There are three important questions: firstly, whether the degradation induced by ambient air affects the stability of all layers of organic solar cells; secondly, whether the degradation can also be induced by the reaction between ambient air and the organic solar cells; and finally, the role of oxygen and/or absorbed water in the degradation.

In this paper, we propose that the degradation of air-process solar cells is caused by the oxidation of interfacial layers and the chemical changes of the active layer. X-ray photoelectron spectroscopy (XPS), time-of-flight secondary ion mass spectrometry (ToF-SIMS), optical spectroscopy, and atomic force microscopy (AFM) were used to characterize the air-processed degradation patterns and failure mechanisms in the organic solar cell. To promote the device processing stability, we need to choose appropriate materials for interfacial layers and the active layer during air operation.

METHOD

Materials

PEDOT:PSS (Clevios Al 4083) was purchased from Heraeus. p-DTS (FBTTh$_2$)$_2$ and PC$_{71}$BM were all purchased from Sigma Aldrich. The solid content of the PEDOT:PSS solution was 1–1.3%, and the weight ratio of PEDOT:PSS is 1:2.5.

Fabrication and Characterization of the OSCs

Photovoltaic devices were prepared with the inverted structure of Glass/ITO/ZnO/active layer/PEDOT:PSS/Ag. Glass slides were cut into 2.5×2.5 cm^2 and cleaned by bath sonication in detergent, DI water, acetone, and isopropanol for 15 min and dried in 90°C oven for 1 h. The substrates were cleaned by a UV/O 4-inch UV/O$_3$ cleaner operating for 20 min. We spin-coated PEDOT:PSS films from solutions on an active layer at 3,000 rpm for 0.5 min. The PEDOT:PSS films were then thermally annealed at 120°C for 15 min on a hotplate. Then, it was slowly cooled to room temperature. The active layer of the p-DTS(FBTTh$_2$)$_2$:PC$_{71}$BM film (PDTS:PCBM$_{71}$) consists of a weight ratio of 6:4 (w/w) solution of 20 mg/ml in chlorobenzene. The active layer is spin-coated on top of the ZnO layer at 800 rpm for 40 s. The electrodes of devices were evaporated by vacuum thermal evaporation (Hex) of 100 nm silver on top of the PEDOT:PSS film through a shadow mask. The photovoltaic performance of the devices was determined using a solar simulator (Keithley 2400) under 100 mW/cm^2 AM 1.5G. The surface morphologies were examined by optical microscopy and atomic force microscopy (AFM, XE-100 system). The structure of the samples was measured using X-ray photoelectron spectroscopy (XPS, Kratos AXIS Ultra DLD instrument with an Al K probe beam).

RESULTS AND DISCUSSION

The structure of the inverted organic solar cell is ITO/ZnO (25 nm)/active layer (65 nm)/PEDOT:PSS (20 nm)/Ag (1,000 nm). The active layers were processed from p-DTS(FBTTh$_2$)$_2$:PC$_{71}$BM solution by spin coating. The current density–voltage characteristics of air-processed OPVs and glove-box-processed OPVs are presented in **Figure 1A**. The OPVs based on p-DTS(FBTTh$_2$)$_2$:PC$_{71}$BM with different processed conditions were fabricated to investigate the degradation effects on device performance. The all-layer glove-box-processed OPV device has a PCE of 6.27% with a Voc (open-circuit voltage) of 0.79 V, Jsc (short-circuit current density) of 18.05 mA/cm^2, and FF (fill factor) of 44%. The PCEs of the OPV devices that were air-processed are all poor compared with the glove-box-processed OPV. The performance of all layer air-processed OPV and the only active layer air-processed OPV are the two worst. They have a Voc of 0.2 V, Jsc of 3 mA/cm^2, and PCE around 0.2%, which are of no use. It can be inferred that the degradation of active layers in the air is responsible for the damage of these two OPVs. The only PEDOT:PSS air-processed OPV also went through huge efficiency loss, which showed a 37% decrement compared with the glove-box-processed OPV. The efficiency loss is mainly derived from the decrease in Jsc of about 30%. The reduction of Jsc is related to the poor transport properties of the photo-generated charge carriers and a continuous pathway in the organic domain, which caused the decline in the conductivity of PEDOT:PSS. The degradation mechanism of PEDOT:PSS in the air leads to big efficiency drops but that are not fatal to the degradation of the active layer.

The XPS was carried out to investigate the air-processed degradation of organic solar cells. The binding energy (BE) obtained in the XPS analysis was corrected by specimen charge by benchmarking the C1s peak to 284.6 eV. First, we perform the XPS on the top layer of the OSCs, which is the layer of PEDOT:PSS. **Figure 1** shows the high-resolution spectrum of C1s, O1s, and S2p (the PEDOT:PSS layer) of glove-box-processed and all layer air-processed OSCs. In **Figure 1B**, there is no obvious difference between the C–C bond spectra of the two OSCs. However, there are fewer C–S and C–O bonds in glove-box-processed OSCs than the air-processed OSCs. In **Figure 1D**, the O1s spectra follow the same trend as the C1s spectra. With the multipeak fitting procedure, the O1s spectra can be resolved by using two spectral components centered at different BE: O–C (BE = 531 eV), O–S, and adsorbed OH bonds (BE = 532.5 eV). There are more O–S and OH bonds in air-processed OSCs than glove-box processed OSCs.
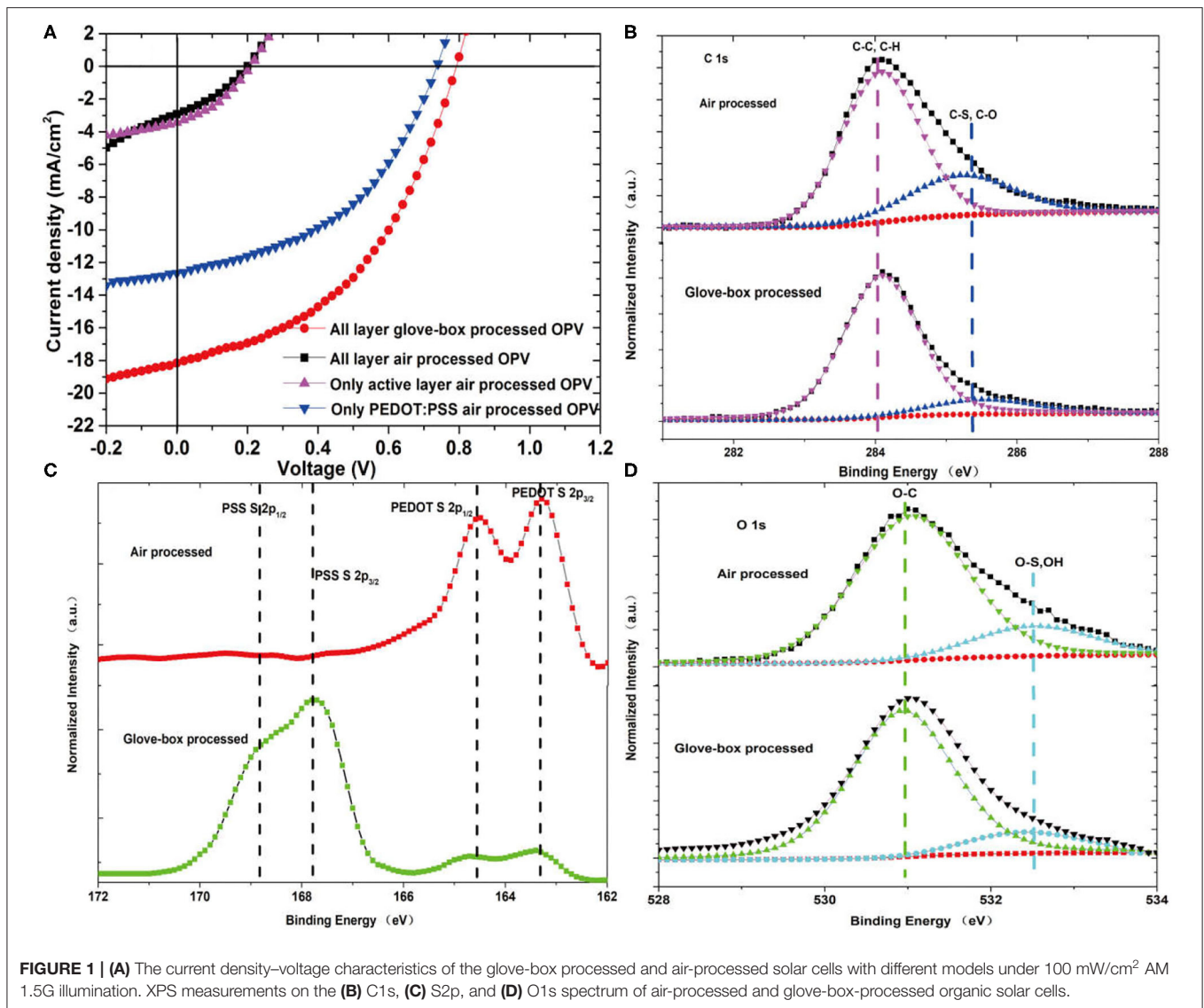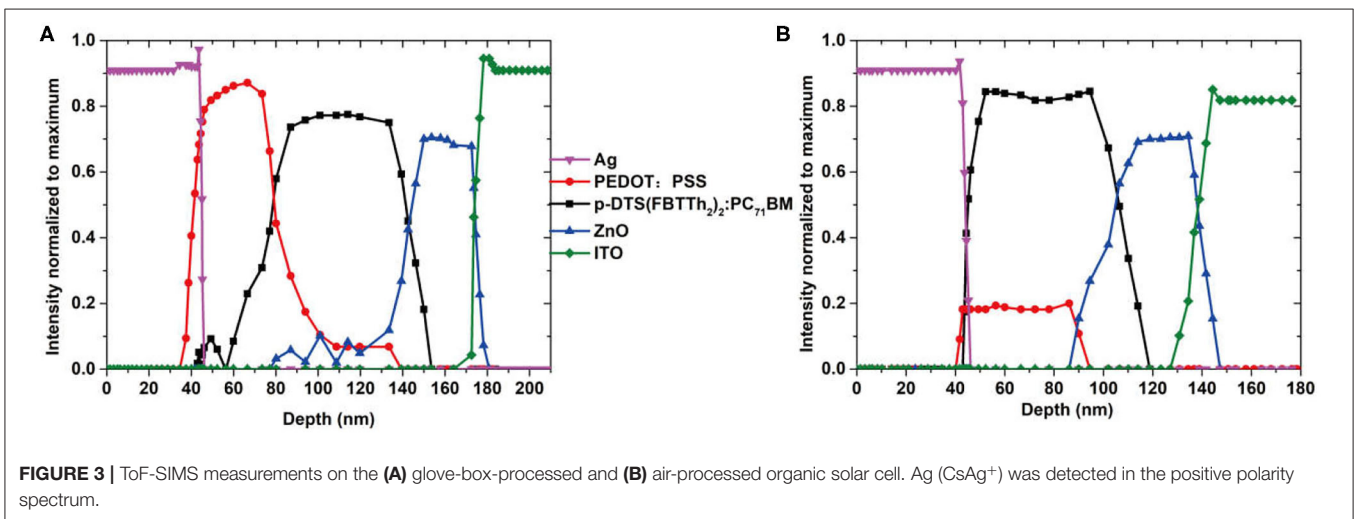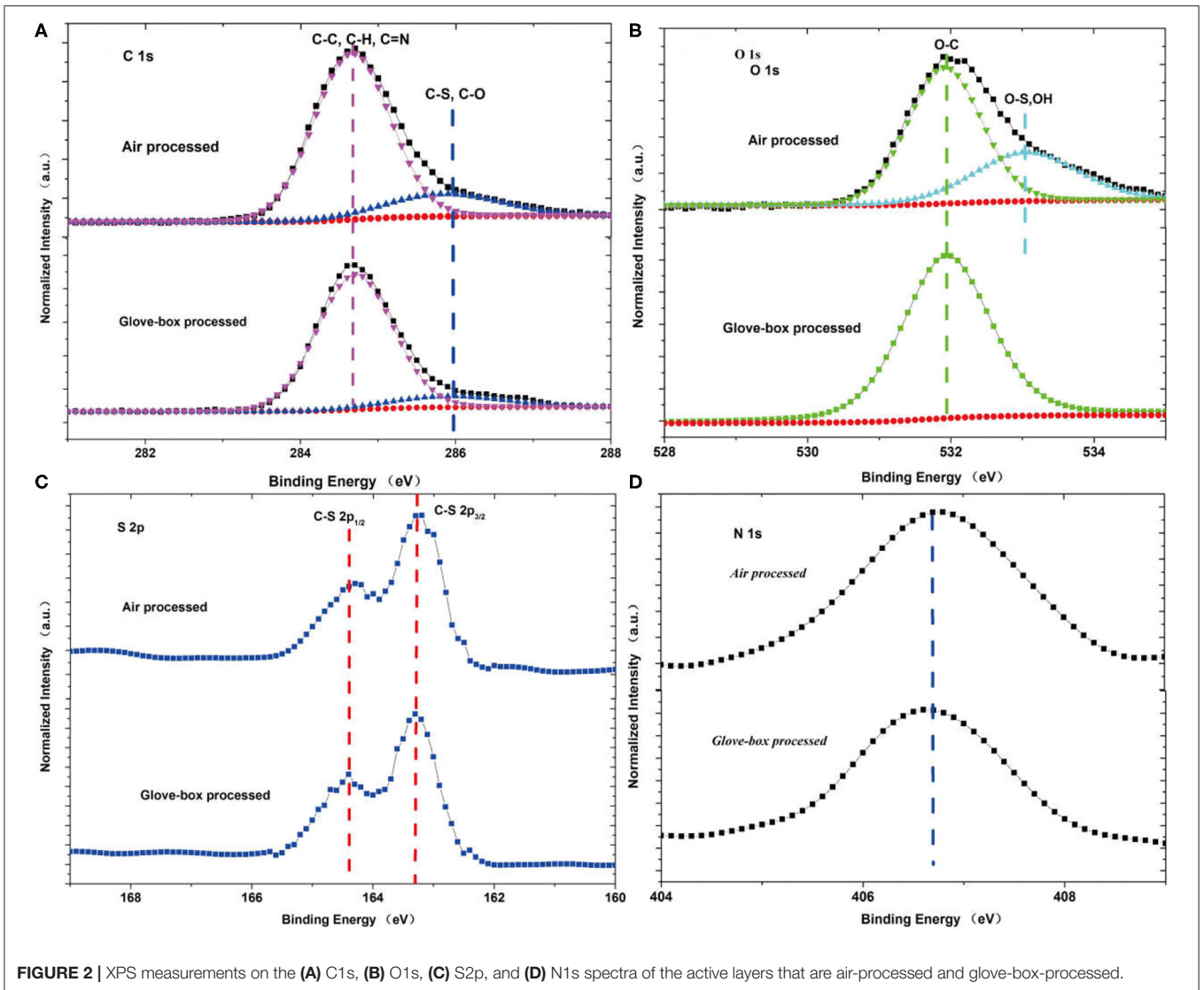
FIGURE 1 | (A) The current density–voltage characteristics of the glove-box processed and air-processed solar cells with different models under 100 mW/cm^2 AM 1.5G illumination. XPS measurements on the **(B)** C1s, **(C)** S2p, and **(D)** O1s spectrum of air-processed and glove-box-processed organic solar cells.

Figure 1C presents the S (sulfur) 2p spectrum of the PEDOT:PSS of glove-box-processed and air-processed organic solar cells. The S 2p spectrum of glove-box-processed OSCs shows a typical S spectra of PEDOT:PSS. The higher binding energy peaks are at 168.8 and 167.8 eV, corresponding to the S atoms in PSS, and the lower binding energy peaks are at 164.6 and 163.3 eV corresponding to the S atoms in PEDOT. The atomic fundamental parameters of sulfur were taken from X-ray lib [13], and these peak values coincide with previous reports [14, 15]. In **Figure 1C**, the O–S bond in the S 2p spectrum of air-processed OSCs was not observed, which indicates no signal of S atoms of PSS. The missing of the PSS signal leads to a conclusion that PSS undergoes a so-called oxido-de-sulfonato-substitution forming the phenolate. This observation indicates that PEDOT:PSS can be oxidized by oxygen and leads to the damage of the OSCs. We note that PEDOT:PSS is synthesized with a small excess of PSS. Oxygen diffuses into the PEDOT:PSS layer and reacts with the

excess PSS. Oxidation of PSS by ambient air is expected mainly to take place at the PSS domain.

In order to further investigate the chemical changes of the active layer in air, we also carry out the X-ray photoemission spectroscopy on the glove-box-processed and air-processed active layers, which is shown in **Figure 2**. In **Figure 2A**, the C1s of the air-processed active layer contains more C–S and C–O bonds than that of the glove-box-processed active layer. In **Figure 2B**, there are many absorbed hydroxyl (OH bond) and H$_2$O in the O1s spectrum of the air-processed active layer, but there is none in the O1s spectrum of the glove-box-processed active layer. Hydroxyl is usually the result of decomposition of water molecules. We infer that the absorbed hydroxyl and H$_2$O tend to immerse into the small-molecule material of p-DTS(FBTTh$_2$)$_2$ and cause the crystallization of the small molecules. In **Figures 2C,D**, no obvious change in the spectra of S 2p and N 1s was found, i.e., the binding
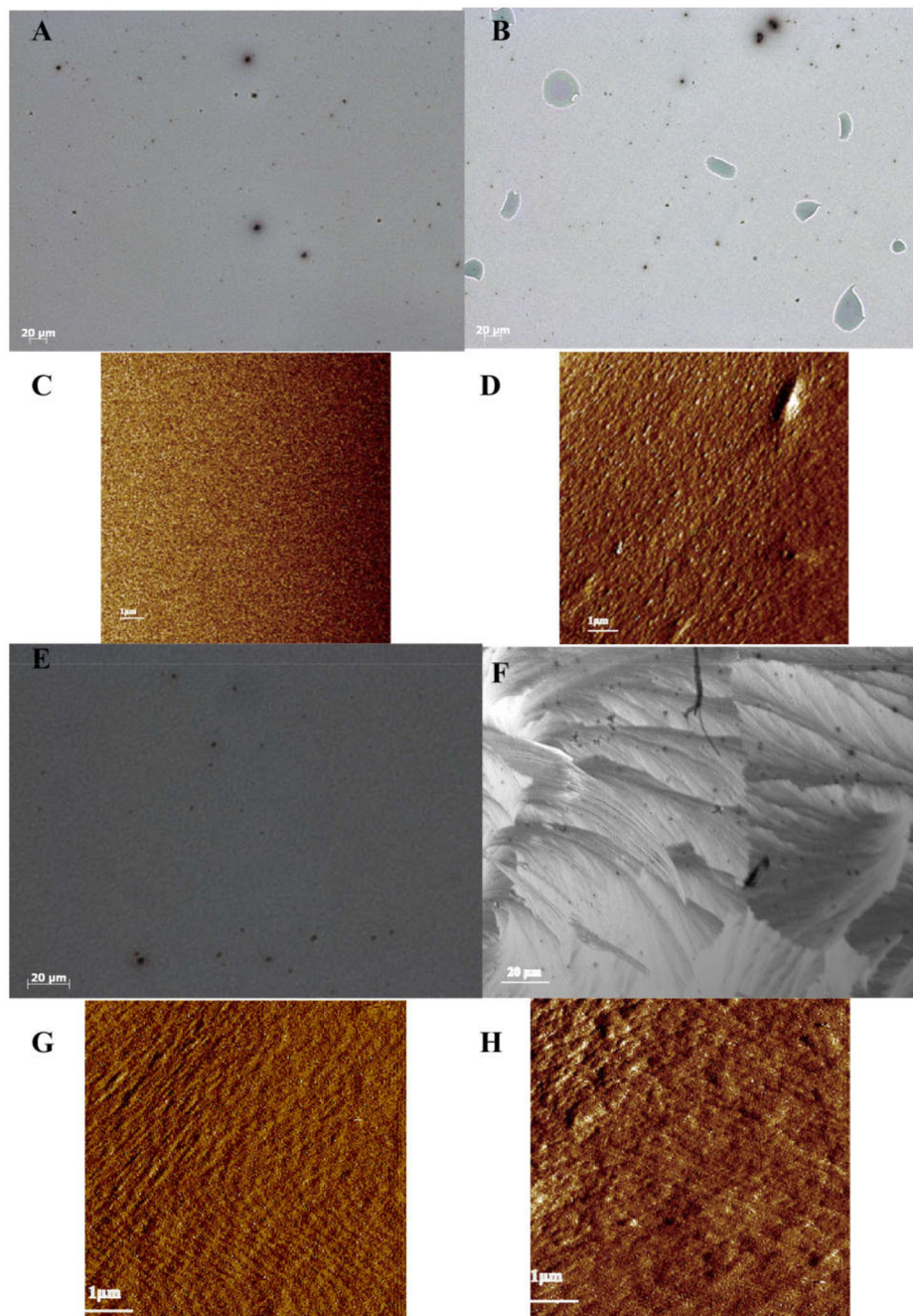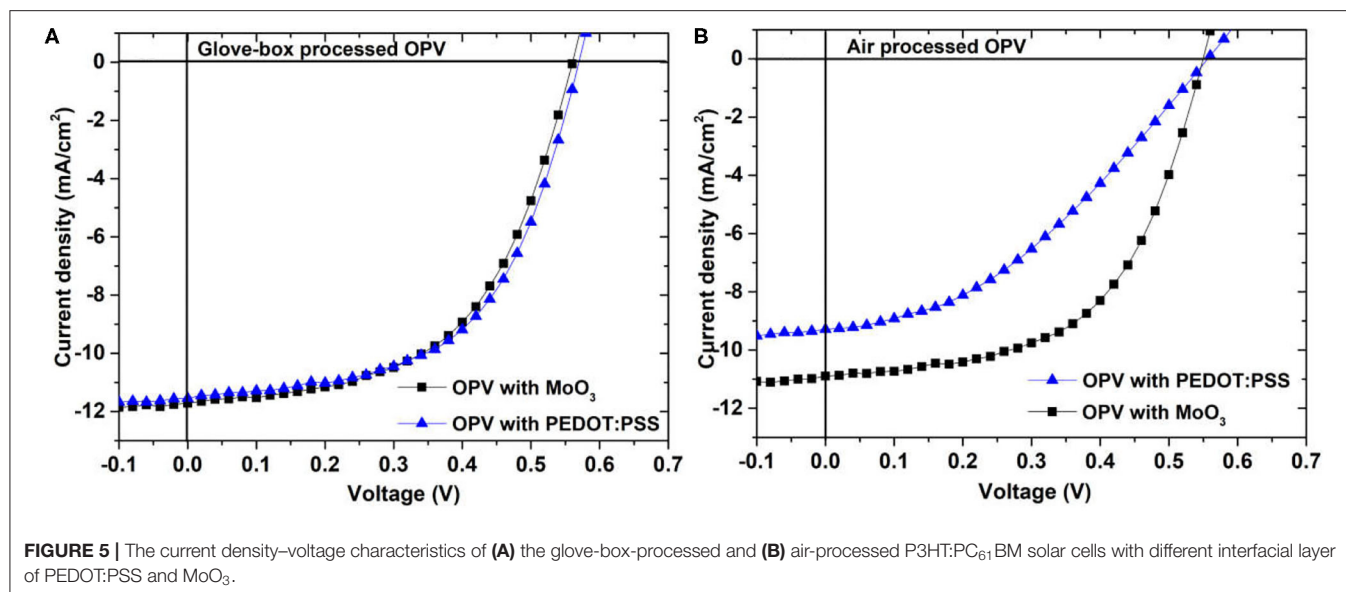
FIGURE 2 | XPS measurements on the **(A)** C1s, **(B)** O1s, **(C)** S2p, and **(D)** N1s spectra of the active layers that are air-processed and glove-box-processed.

FIGURE 3 | ToF-SIMS measurements on the **(A)** glove-box-processed and **(B)** air-processed organic solar cell. Ag (CsAg⁺) was detected in the positive polarity spectrum.

FIGURE 4 | High-resolution optical microscope of PEDOT:PSS surfaces processed **(A)** in glove-box and **(B)** in air; AFM images of PEDOT:PSS surfaces processed **(C)** in glove-box and **(D)** in air; OM images of p-DTS(FBTTh$_2$)$_2$:PC$_{71}$BM surfaces **(E)** in glove-box and **(F)** in air; AFM images of p-DTS(FBTTh$_2$)$_2$:PC$_{71}$BM surfaces processed **(G)** in glove-box and **(H)** in air.

energy of peak positions and the spectral shapes appear to be essentially the same between the air-processed and glove-box-processed OSCs.

Further evidence was obtained from time-of-flight secondary ion mass spectroscopy (ToF-SIMS) measurements. During ToF-SIMS measurements, the layers were successively ablated with a Cs$^+$ ion beam while positively and negatively charged ions were detected. The ToF-SIMS signal and the corresponding layers of the solar cell are shown in **Figure 3A**, where the intensity of all signals was normalized to one. The signals of p-DTS(FBTTh$_2$)$_2$:PC$_{71}$BM, ZnO, ITO, and Ag of the air-processed and glove-box-processed OSCs are virtually identical. In **Figure 3B**, the signal of PEDOT:PSS is not only very weak but also merges into the one of the

FIGURE 5 | The current density–voltage characteristics of **(A)** the glove-box-processed and **(B)** air-processed P3HT:$PC_{61}BM$ solar cells with different interfacial layer of PEDOT:PSS and MoO_3.

p-DTS(FBTTh$_2$)$_2$:PC$_{71}$BM active layer. This clear observation indicated that PEDOT:PSS has undergone some chemical changes in the air due to the process of oxidation and desulfurization of PEDOT:PSS. The result of ToF-SIMS accords with the XPS data of PEDOT:PSS.

Figure 4 shows the surfaces of the interfacial layers and active layers of the glove-box-processed and air-processed organic solar cells by using high-resolution optical microscopy (OM) and AFM. **Figures 4A,C** present the neat and smooth surface of the glove-box-processed PEDOT:PSS layer of the OSCs by OM and AFM, while in **Figures 4B,D**, many defects can be found in the surface of the air-processed PEDOT:PSS layer. It seems that the PEDOT:PSS layer has undergone a corrosion process by oxygen in the air. The large number of defects can hinder carrier migration leading to a poor conductivity, which coincides with the poor Jsc of the only PEDOT:PSS layer air-processed OPV. The degradation of PEDOT:PSS in air is verified by ToF-SIMS, XPS, high-resolution optical microscopy, and AFM. These results clearly show that PEDOT:PSS underwent a corrosion process by oxygen.

Figures 4E–H present the surface of the active layer of p-DTS(FBTTh$_2$)$_2$:PC$_{71}$BM by optical microscopy and AFM, processed in glove-box and air, respectively. As shown in **Figures 4E,F**, there is a smooth surface in the glove-box-processed p-DTS(FBTTh$_2$)$_2$:PC$_{71}$BM film, while there is a large area of crystalline surface in the air-processed p-DTS(FBTTh$_2$)$_2$:PC$_{71}$BM film. The reason can be attributed to that p-DTS(FBTTh$_2$)$_2$ as a small organic molecule tends to aggregate and crystallize under absorbed water and hydroxyl molecules. The large-area crystalline surface is detrimental to the charge transport, which affects the performance of the solar cell. This is the reason that the air-processed p-DTS(FBTTh$_2$)$_2$:PC$_{71}$BM-based solar cells all failed. In **Figure 4G**, the AFM surface topography shows a flat surface in the glove-box-processed

p-DTS(FBTTh$_2$)$_2$:PC$_{71}$BM film and the root mean square (RMS) value of it is 1.5 nm. However, for the p-DTS(FBTTh$_2$)$_2$:PC$_{71}$BM film processed in the air, the RMS increases to 3.2 nm, as shown in **Figure 4H**. This increase in the RMS value resulted from the crystal nucleation and coalescence of small molecules.

The degradation of PEDOT:PSS in air is hard to avoid, but we can choose another interfacial layer to substitute PEDOT:PSS such as MoO_3. We compared the performance of air-processed and glove-box-processed OPV with PEDOT:PSS and MoO_3. The active layer is P3HT:PC$_{61}$BM. **Figure 5** shows the current density–voltage characteristics of (A) the glove-box-processed and (B) air-processed solar cells with different interfacial layer of PEDOT:PSS and MoO_3 under 100 mWcm^{-2} AM 1.5G illuminations. As processed in glove-box, the performances of the MoO_3 and PEDOT:PSS solar cells are basically the same. However, the performance of the MoO_3 solar cell is better than that of PEDOT:PSS solar cells in air. There is no degradation on the MoO_3 solar cell in air.

CONCLUSIONS

This paper presents the processing degradation mechanism of air-processed organic solar cells for future industrial production. The outcomes of this study demonstrate two main degradation mechanisms of the air-processed organic solar cells:

1) We depicted the processing degradation mechanism of PEDOT:PSS. Based on the results of ToF-SIMS, XPS, and high-resolution optical microscope, it is confirmed that PEDOT:PSS underwent an oxidation and desulfurization process by oxygen and formed a large number of defects, which can hinder charge transfer leading to an inferior performance.

2) We showed the degradation of the p-DTS(FBTTh$_2$)$_2$:PC$_{71}$BM small-molecule active layer in the air. There is a large-area crystalline surface in the p-DTS(FBTTh$_2$)$_2$:PC$_{71}$BM active layer when processed in the air, which is fatal to the organic solar cells. The small molecules of p-DTS(FBTTh$_2$)$_2$ tend to be affected by absorbed hydroxyl and water and transform to aggregated and crystallized surface.

DATA AVAILABILITY STATEMENT

The raw data supporting the conclusions of this article will be made available by the authors, without undue reservation.

AUTHOR CONTRIBUTIONS

MW planned and supervised the experiments and wrote and revised the manuscript. XC, YH, KZ, and FL worked on data processing. All authors contributed to the article and approved the submitted version.

REFERENCES

1. Zhao W, Li S, Zhang S, Liu X, Hou J. Ternary polymer solar cells based on two acceptors and one donor for achieving 12.2% efficiency. *Adv Mater*. (2017) **1**:4059–66. doi: 10.1002/adma.201604059

2. Yuan J, Zhang Y, Zhou L, Zhang G, Yip H-L, Lau T-K, et al. Single-junction organic solar cell with over 15% efficiency using fused-ring acceptor with electron-deficient core. *Joule*. (2019) **3**:1140–51. doi: 10.1016/j.joule.2019.01.004

3. Nian L, Kan Y, Wang H, Gao K, Xu B, Rong Q, et al. Jen ternary non-fullerene polymer solar cells with 13.51% efficiency and a record-high fill factor of 78.13%. *Energy Environ Sci*. (2018) **11**:3392–9. doi: 10.1039/C8EE 01564C

4. Cheng P, Zhang M, Lau T-K, Wu Y, Jia B, Wang J, et al. Realizing small energy loss of 0.55 eV, high open-circuit voltage >1 V and high efficiency >10% in fullerene-free polymer solar cells via energy driver. *Adv Mater*. (2017) **19**:16052161. doi: 10.1002/adma.201605216

5. Xu X, Feng K, Bi Z, Ma W, Zhang G, Peng Q. Single-junction polymer solar cells with 16.35% efficiency enabled by a platinum(II) complexation strategy. *Adv Mater*. (2019) **31**:e1901872. doi: 10.1002/adma.2019 01872

6. Seemann A, Sauermann T, Lungenschmied C, Armbruster O, Bauer S, Egelhaaf H-J, et al. Reversible and irreversible degradation of organic solar cell performance by oxygen. *Sol Energy*. (2011) **85**:1238–49. doi: 10.1016/j.solener.2010.09.007

7. Norrman K, Madsen MV, Gevorgyan SA, Krebs FC. Degradation patterns in water and oxygen of an inverted polymer solar cell. *J Am Chem Soc*. (2010) **132**:16883–92. doi: 10.1021/ja106299g

8. Chen Z, Xu Y-J. Ultrathin TiO2 layer coated-CdS spheres core–shell nanocomposite with enhanced visible-light photoactivity. *ACS Appl Mater Interfaces*. (2013) **12**: 3792–9. doi: 10.1021/am4043068

9. Baran D, Ashraf RS, Hanifi DA, Abdelsamie M, Gasparini N, Röhr JA, et al. Reducing the efficiency–stability–cost gap of organic photovoltaics with highly efficient and stable small molecule acceptor ternary solar cells. *Nat Commun*. (2016) **10**:1038. doi: 10.1038/nmat4797

10. Cheng P, Zhan X. Stability of organic solar cells: challenges and strategies. *Chem Soc Rev*. (2016) **9**:2544–82. doi: 10.1039/C5CS00593K

11. Kang Q, Ye L, Xu B, An C, Stuard SJ, Zhang S, et al. A printable organic cathode interlayer enables over 13% efficiency for 1 cm^2 organic solar cells. *Joule*. (2019) **3**:227–39. doi: 10.1016/j.joule.2018.10.024

12. Dong S, Zhang K, Jia T, Zhong W, Wang X, Huang F. Suppressing the excessive aggregation of nonfullerene acceptor in blade-coated active layer by using n-type polymer additive to achieve large-area printed organic solar cells with efficiency over 15%. *EcoMat*. (2019) **1**:e12006. doi: 10.1002/eom2.12006

13. Schoonjans T, Brunetti A, Golosio B, Sanchez del Rio M, Solé VA, Ferrero C, et al. The xraylib library for X-ray–matter interactions. Recent developments. *Spectrochim Acta B*. (2011) **66**:776–84. doi: 10.1016/j.sab.2011.09.011

14. Alemu D, We H-Y, Ho KC, Chu CW. Highly conductive PEDOT:PSS electrode by simple film treatment with methanol for ITO-free polymer solar cells. *Energy Environ Sci*. (2012) **5**:9662–71. doi: 10.1039/c2ee22595f

15. Na S-I, Wang G, Kim S-S, Kim T-W, Oh S-H, Yu B-K, et al. Evolution of nanomorphology and anisotropic conductivity in solvent-modified PEDOT:PSS films for polymeric anodes of polymer solar cells. *J Mater Chem*. (2009) **19**:9045–53. doi: 10.1039/b915756e